MODELLING OF THERMAL BEHAVIOUR OF POLYMER INSULATION AT HIGH ELECTRIC DC FIELD

C. O. Olsson
ABB Corporate Research, Västerås, Sweden

Abstract

The temperature distribution in polymer insulation of high voltage direct current cables has been studied with a numerical model. The model includes coupling between the electric field distribution and the temperature due to heat generation by the electric current passing through the insulation. The electrical conductivity is a function of temperature and electric field, and at sufficiently high electric field the heating starts to accelerate. Simulation results are presented for cables subjected to stepwise increasing voltage for two different insulation materials with and without heat generation in the conductor.

1 Introduction

The use of polymers as electrical insulation in high voltage equipment is increasing due to cost reasons and due to their good environmental performance. One specific application is the use of extruded polymers for high voltage DC cables, which are installed for e.g. offshore windfarm connections, undergrounding, and subsea interconnections.

The electric field distribution in a DC cable is mainly governed by the electrical conductivity, which is a temperature dependent property. The conductivity also depends on the electric field and on the local composition of the insulation material. At sufficiently high conductivity and electric field, the heat generation due to the current passing through the insulation might be significant.

A one-dimensional transient model has been setup in order to study the distribution of temperature and electric field in a simple cable structure. The temperature influences the electric field distribution through the conductivity and the electric field influences the temperature distribution through resistive heating. A heat flux through the insulation layer might also exist due to heat generation in the conductor at the centre of the cable. The heat conduction equation contains a source term that depends on the conductivity and the electric field. The equations needed in order to solve for the electric field distribution are the Maxwell equations for weakly conducting materials, and these equations are solved with full coupling to the heat conduction equation.

The coupling between temperature distribution and electric field distribution in polymer insulation for high voltage direct current is recognized as an important issue and a large number of publications have been presented during the last 20 years. Early publications on the electric field distribution in DC cables are e.g. Pugliese (1950), Tellier et al. (1958), and Lau (1970). The insulation material was oil impregnated paper and the non-uniform electric field distribution due to the geometry and due to the radial temperature gradient was shown. Olshausen and Sachs (1982) investigated the electrical conductivity of polyethylene which is now used as insulation in high voltage cables. Measurements of conductivity as function of temperature and electric field were presented, and hypotheses on the physical mechanisms governing the conductivity were discussed. Aladenize et al. (1997) describe an analytical model for the time dependent distribution of electric field. In this model the temperature distribution is fixed in time and the electric field develops from

the initially capacitive distribution at voltage application to the steady-state resistive distribution. The conductivity was considered as a function of temperature and electric field.

Results from numerical simulations of the electric field distribution using temperature and field dependent electrical conductivities were presented in Boggs et al. (2001) and Boggs (2004). Formulas for electrical conductivity were presented for two different grades of polymer insulation, one that has comparatively small temperature dependence and large electric field dependence (A) and another that has large temperature dependence and small electric field dependence (B). The first was described as good whereas the second was considered bad based on the resulting electric field distribution in a cable with a large temperature gradient. However, as will be seen in the present investigation, material A provides higher electrical conductivity than material B, and when resistive heating due to the current through the insulation is included in the model the first material can not withstand as high electric field as the second material. Bodega (2006) presented numerical simulations as well as measurements on the electric field distribution accounting for the influence of temperature and electric field of the electrical conductivity of polymer insulated cables.

In the present investigation, electrical conductivities given in Boggs et al. (2001) will be used to describe the insulation material; however there are several other publications that give valuable information on the electrical properties of polymer insulation for DC applications, e.g. Lewis (2002), Boström et al. (2002), Hanley et al. (2003), Ildstad et al. (2004), and Chong et al. (2007).

2 Numerical model

The thermal behaviour of a polymer insulated cable at high electric DC field will be studied. The cable is assumed to consist of the following cylindrical layers: an aluminium conductor of 10 mm radius, a conductor screen of 1 mm thickness, an 8 mm insulation layer, an insulation screen of 1 mm thickness, a 3 mm lead layer, and a polymer oversheath of 2 mm thickness. The outer radius of the cable is thus 25 mm. This geometry has the same dimensions as the cable described in Olsson (2006). Only the conductor material is different.

The electric field distribution is modelled assuming that the insulation material can be considered as a weakly conducting material, see e.g. Dissado and Fothergill (1992). The relevant Maxwell equations are the following.

Electric field: $$E = -\nabla V \tag{1}$$

Electric current density: $$j = \sigma E \tag{2}$$

Space charge: $$\rho_e = \nabla \cdot (\varepsilon_0 \varepsilon_r E) \tag{3}$$

Current continuity: $$\nabla \cdot j = -\frac{\partial \rho_e}{\partial t} \tag{4}$$

The space charge ρ_e can be expressed in terms of electric current density and material properties by inserting equations (2) and (4) in equation (3):

$$\rho_e = -\frac{\varepsilon_0 \varepsilon_r}{\sigma} \frac{\partial \rho_e}{\partial t} + j \cdot \nabla \left(\frac{\varepsilon_0 \varepsilon_r}{\sigma} \right) \tag{5}$$

The electric field can be obtained from solving equations (1-3), and (5) in which the voltage V, the electric field E, the current density j, and the space charge ρ_e are the unknown variables. The

electrical properties that are included in the model are the permittivity of vacuum ε_0, the relative permittivity of the insulation ε_r, and the electrical conductivity σ. The relative permittivity is approximately $\varepsilon_r = 2.3$ for olefinic polymers. The relative permittivity is much less sensitive to temperature and electric field as compared to the conductivity σ, and for simplicity ε_r is assumed constant.

The temperature distribution is given by the heat conduction equation.

$$\rho_m c_p \frac{\partial T}{\partial t} = \nabla \cdot (k \nabla T) + S_{heat} \tag{6}$$

A source term is included in order to account for resistive heating due to the current that passes through the insulation.

$$S_{heat} = \frac{|j|^2}{\sigma} = \sigma |E|^2 \tag{7}$$

The second equality follows from equation (2). Heat generation can also take place in the conductor of the cable.

The electrical conductivity of the insulation material can be a function of composition, temperature, and electric field.

$$\sigma = \prod_i f_{c_i}(c_i) f_T(T) f_E(E) \tag{8}$$

The composition of an insulation material can be a function of temperature and time due to diffusion of various substances, see Olsson (2006). However, in this study the composition is assumed to be uniform, i.e.

$$\prod_i f_{c_i}(c_i) = 1 \tag{9}$$

The influence of temperature and electric field is taken from Boggs et al. (2001). Two different insulation materials, A and B, will be considered, and the conductivities are given by the following formulas, see also Figure 1.

$$\sigma_A = 3.2781 e^{-\left(\frac{0.56 q_E}{k_B T}\right)} \frac{\sinh\left(2.7756 \times 10^{-7} |E|\right)}{|E|} \quad \text{[S/m]} \tag{10}$$

$$\sigma_B = 3.6782 \times 10^7 e^{-\left(\frac{0.98 q_E}{k_B T}\right)} \frac{\sinh\left(1.086 \times 10^{-7} |E|\right)}{|E|} \quad \text{[S/m]} \tag{11}$$

In equations 10 and 11, q_E and k_B are the charge of the electron and the Boltzmann constant, respectively, and the values 0.56 and 0.98 are activation energies in eV units.

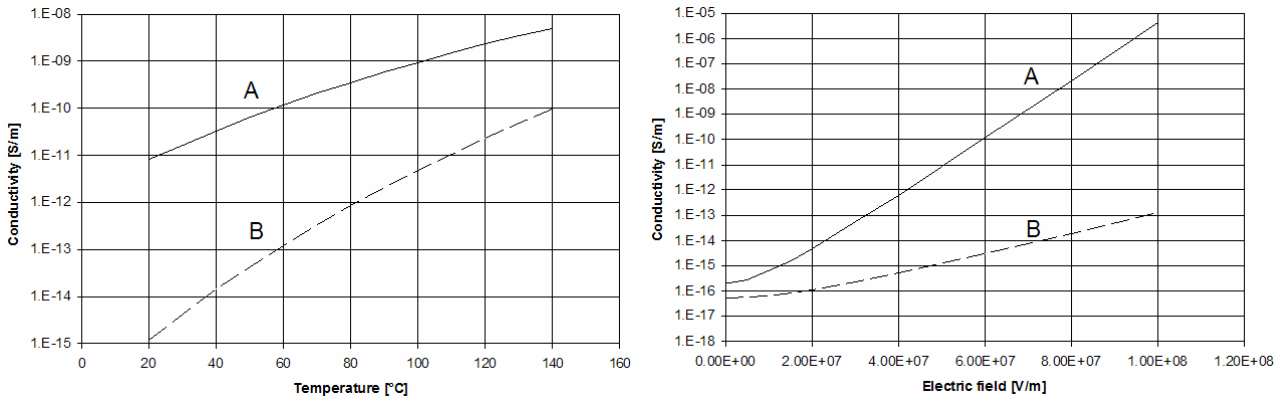

a b

Figure 1: *Electrical conductivity for materials A and B. a) Temperature dependence at* $E = 5.0 \times 10^7$ *V/m and b) electric field dependence at* $T = 20$ °C.

The thermal properties of the insulation materials are assumed to be the same as those used in Olsson (2006), and the specific heat and the thermal conductivity depend on temperature. The thermal properties of the aluminium conductor are assumed to be $\rho = 2700$ kg/m³, $c_p = 890$ J/kgK, and $k = 200$ W/mK. The lead layer has the following thermal properties: $\rho = 11340$ kg/m³, $c_p = 125$ J/kgK, and $k = 35$ W/mK.

For the electrical problem, boundary conditions are needed for the voltage V and for the current density j. At each side of the insulation layer the voltage is specified. The conductor screen is assumed to be at voltage V_0 which could be a function of time. At the insulation screen, the voltage is assumed to be zero. The current density at the insulation interfaces is given by the electric field and the conductivity at the interfaces according to equation (2). This is a simplification since the current density can be a non-linear function of the electric field and can also depend on the electrode material and the voltage polarity, see e.g. Dissado and Fothergill (1992).

The thermal boundary condition on the outer surface of the cable is dictated by free convection and thermal radiation as in Olsson (2006). When heat generation in the conductor is considered, the heat source is set to 1.75×10^5 W/m³ which corresponds to a conductor temperature of approximately 70 °C at steady-state when the ambient temperature is 20 °C.

The equations described above have been solved using the finite element program Comsol Multiphysics, version 3.3, which enables simultaneous solution of several coupled differential equations. A one-dimensional transient model is used, and the heat conduction equation is solved from the centre line of the conductor to the cable surface whereas the electrical problem is solved only within the insulation layer. The second order finite element mesh consists of approximately 1200 elements of which 400 are located within the 8 mm thick insulation layer.

3 Results and discussion

The development of temperature distribution and electric field distribution has been studied for material A and material B with and without conductor heating. The voltage at the conductor V_0 is increased in steps until the temperature of the insulation becomes unstable due to accelerated heat generation by the current passing through the insulation. At start, $t = 0$ s, V_0 is set to 8×10^4 V, and the insulation is free from space charge and the temperature is uniform at the ambient temperature 20 °C. If conductor heating is included, the heating starts at $t = 0$ s. The first voltage level is kept for 3600 s, and subsequently V_0 is increased 4×10^4 V each 1200 s. A voltage increase is given as a

linear ramp of V_0 during 60 s. The simulations have been ended when the temperature increase in the insulation is approximately 10 K/s.

In Figure 2, the temperature difference between the middle point of the insulation layer and the ambient is shown for material A without conductor heating. A logarithmic scale is chosen for the vertical axis in order to clearly show the small temperature increase during the first steps. After each voltage increase the temperature increases and tends toward a steady-state value until the voltage is increased again; however 1200 s is not sufficient to reach the steady-state.

In Figures 3a and 3b, the development with time of electric current density and electric field, respectively, are shown. Three curves are shown in each graph representing the inside interface r = 0.011 m, the middle r = 0.015 m, and the outside interface of the insulation layer r = 0.019 m. For each voltage step, the current density increases, and during a period with constant conductor voltage the current density decreases in the inner part of the insulation whereas it increases in the outer part. This is due to the electric field dependence of the conductivity that makes the conductivity non-uniform in a cylindrical layer, and according to equation (5) space charge will be accumulated when there is a gradient in conductivity. At 8400 s, the voltage is increased to 2.8×10^5 V corresponding to an average electric field of 3.5×10^7 V/m, and at this level the conductivity is sufficiently high to make the current density steady almost immediately after the voltage increase. After the last voltage increase to $V_0 = 4.4 \times 10^5$ V, i.e. $E_{avg} = 5.5 \times 10^7$ V/m, the current density shows an accelerating increase which leads to unlimited heating of the insulation. If the voltage had been kept constant for longer time at each level, the accelerating heating would take place already at the step before, i.e. $V_0 = 4.0 \times 10^5$ V and $E_{avg} = 5.0 \times 10^7$ V/m. The distribution of the electric field is modified during the first steps such that the field decreases in the inner part and increases in the outer part of the insulation layer. At each new voltage step, a capacitive field is added to the field distribution attained during the previous step, and with time the field adjusts to the resistive distribution dictated by the conductivity distribution. When the heating becomes accelerating, the electric field distribution undergoes a dramatic change due to the temperature gradient in the insulation layer. The electric field decreases in the hottest part and increases in the colder parts close to the insulation interfaces. The radial temperature distribution for each second during the last ten seconds of the simulation is shown in Figure 3c, and the electric field distribution is shown in Figure 3d. It can be seen that the electric field is pushed away from the central part of the insulation toward the interfaces. The thermal inertia of the conductor and the lead layer concentrates the accelerating heating to the inner part of the insulation layer.

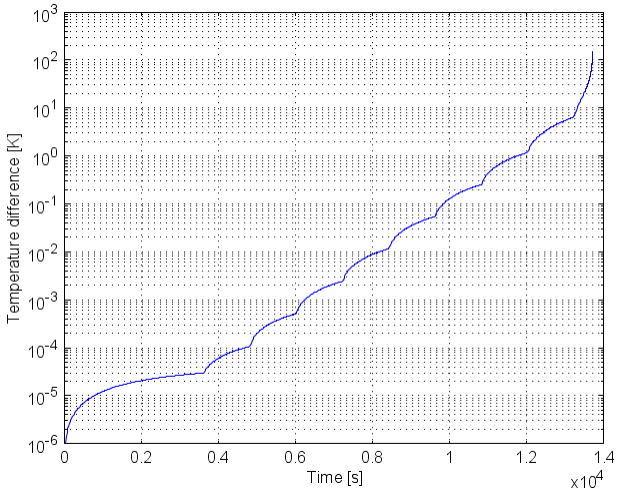

Figure 2: *Temperature difference between middle of insulation and ambient for material A without conductor heating. Logarithmic temperature scale.*

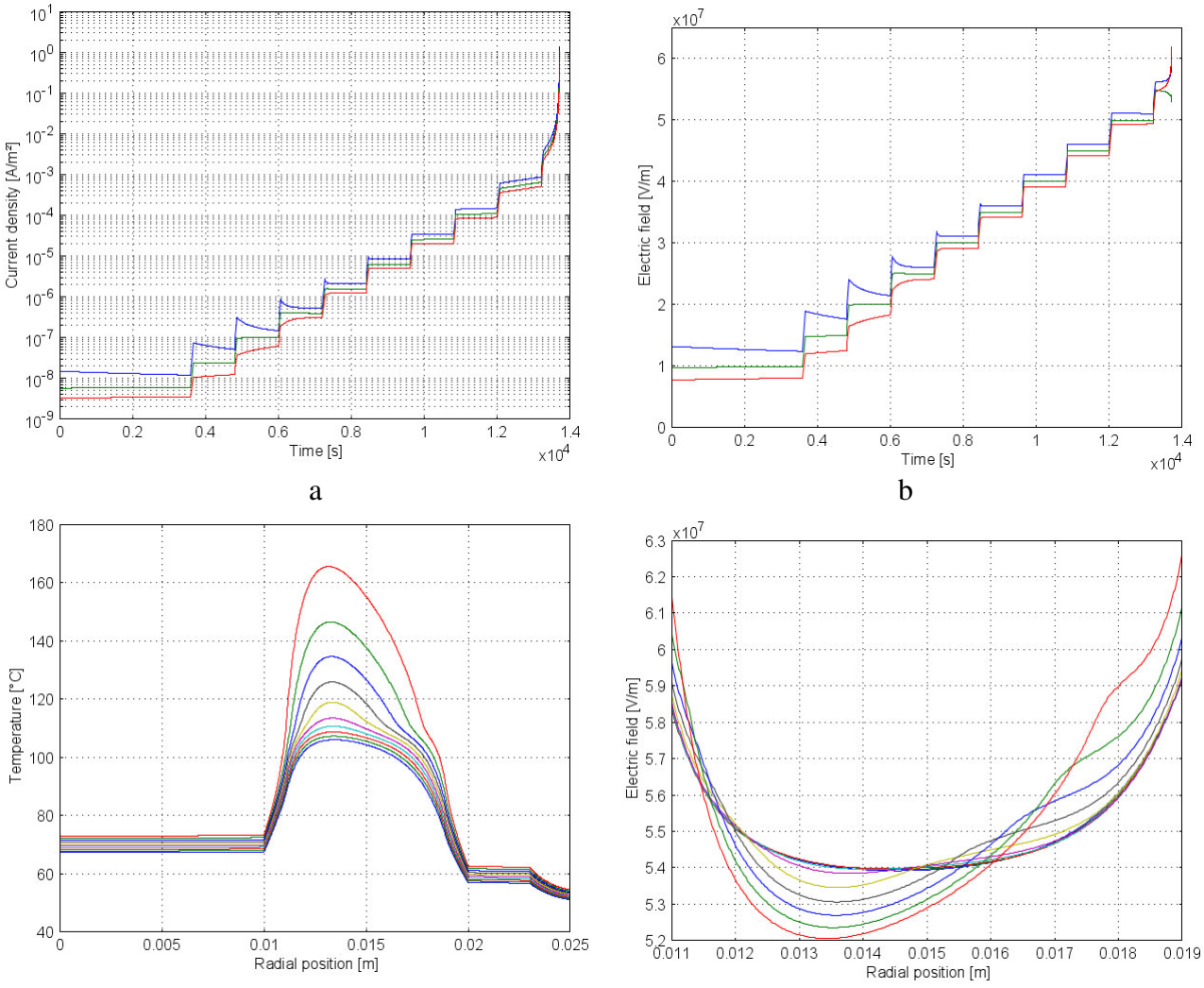

Figure 3: *Material A without conductor heating. a) Electric current density vs. time and b) electric field vs. time; blue, green, and red lines represent, r = 0.011, 0.015, and 0.019 m, respectively. c) Temperature profiles and d) electric field profiles each second during the last ten seconds.*

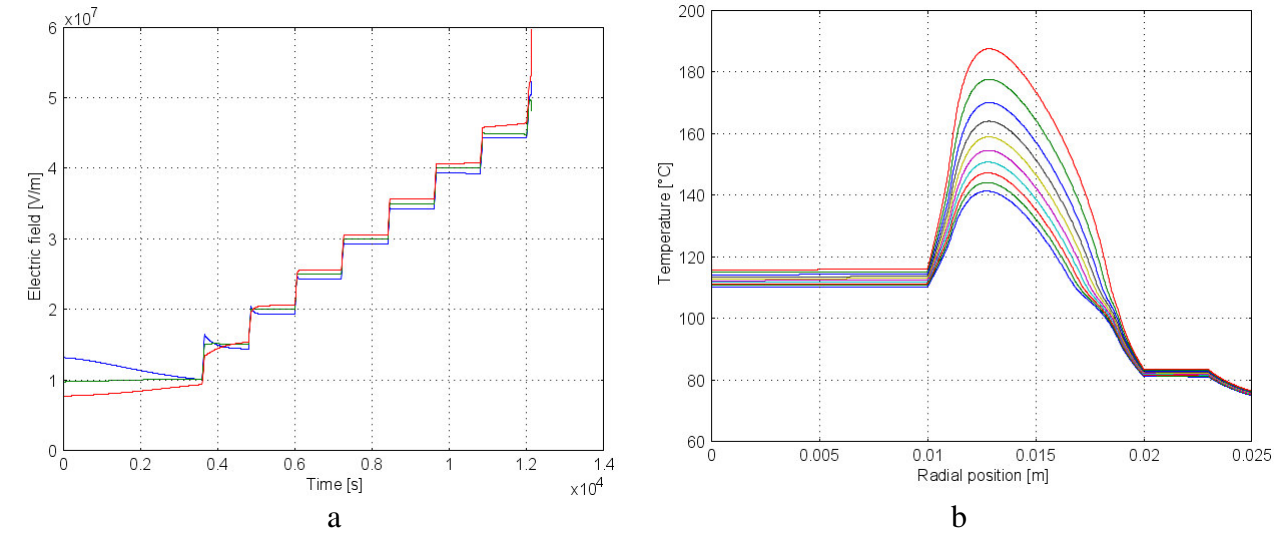

Figure 4: *Material A with conductor heating. a) Electric field vs. time; blue, green, and red lines represent r = 0.011, 0.015, and 0.019 m, respectively. b) Temperature profiles each second during the last ten seconds.*

In Figure 4, simulation results are shown for material A with conductor heating. For this case a radial temperature gradient develops due to the heat generation in the conductor, and the associated gradient in electrical conductivity makes the resistive electric field increase with increasing radius in the insulation layer. The electric field is thus inverted from the capacitive to the resistive distribution, and in Figure 4a it is seen that the curve for r = 0.011 m crosses the curve for r = 0.019 m at t = 4100 s. After the last voltage increase to $V_0 = 4.0 \times 10^5$ V, i.e. $E_{avg} = 5.0 \times 10^7$ V/m, the current density shows an accelerating increase which leads to unlimited heating of the insulation. If the voltage would have been kept constant for longer time at each level, the accelerating heating would take place already at the step before, i.e. $V_0 = 3.5 \times 10^5$ V and $E_{avg} = 4.5 \times 10^7$ V/m. The change in temperature distribution during the last ten seconds of the simulation as shown in Figure 4b indicates slower acceleration in the heating as compared to the corresponding graph in Figure 3c.

Results for material B are shown without conductor heating in Figure 5a and with conductor heating in Figure 5b. Since material B has lower electrical conductivity than material A, a higher voltage is reached before the accelerated heating takes place. Without conductor heating, $V_0 = 1.0 \times 10^6$ V and $E_{avg} = 1.25 \times 10^8$ V/m at the end of the simulation and with conductor heating the corresponding values are $V_0 = 7.2 \times 10^5$ V and $E_{avg} = 9.0 \times 10^7$ V/m. Material B has a conductivity that is more dependent on temperature and less dependent on electric field as compared to material A. The consequences of this are seen in the graphs showing the electric field as function of time. For material B without conductor heating, the electric field at which the resistive field distribution is rapidly obtained after a voltage increase is much higher than for material A. It was also found that when the simulation was ended for material B without conductor heating, the conductor had attained approximately 50 °C whereas the conductor temperature was almost 70 °C at the end of the simulation for material A without conductor heating. It seems thus as material B provides a more sudden acceleration in heating as compared to material A which is probably due to the smaller electric field dependence of the conductivity of material B. The development of temperature and electric field distributions for the cases with conductor heating are rather similar for both materials; however the average electric field at accelerating heating is much higher for material B.

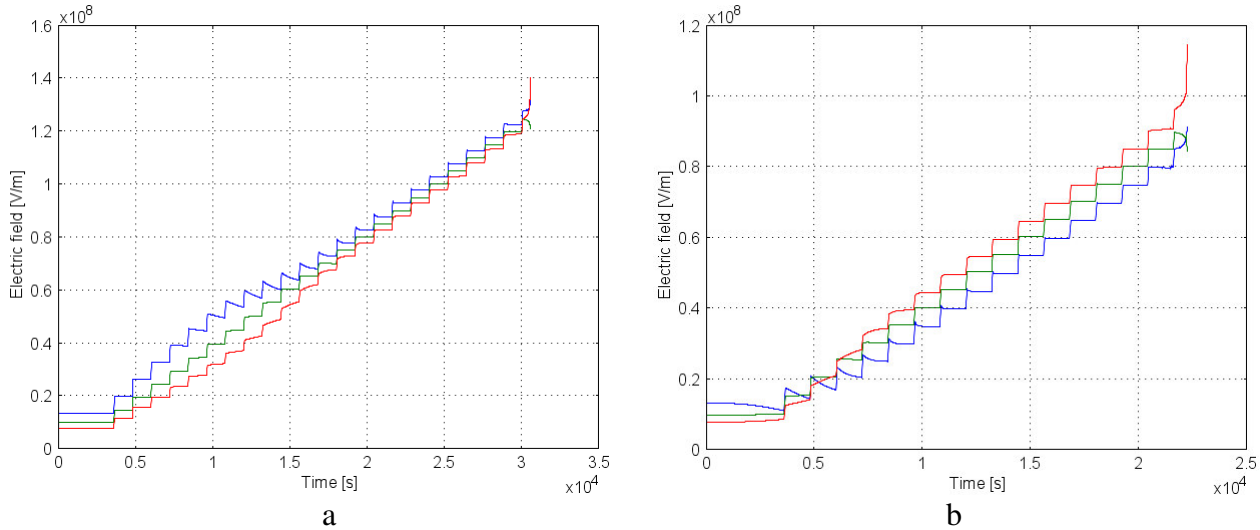

Figure 5: *Electric field vs. time for material B. a) Without conductor heating and b) with conductor heating. Blue, green, and red lines represent r = 0.011, 0.015, and 0.019 m, respectively.*

4 Conclusions

A numerical model of temperature and electric field for direct current electrical insulation has been developed including the heating due to the electric current passing through the insulation. The thermal behaviour of polymer insulated cables subjected to stepwise increasing voltage has been investigated for two different insulation materials with and without heat generation in the conductor at the centre of the cable.

At sufficiently high electric field, the heating in the insulation becomes accelerating due to the temperature dependence of the electrical conductivity. Details of the temperature distribution and electric field distribution can be studied with the presented model.

5 References

Aladenize, B., Coelho, R., Guillaumond, F., and Mirebeau, P., On the intrinsic space charge in a dc power cable, J. Electrostatics., 39, pp. 235-251, 1997.

Bodega, R., Space charge accumulation in polymeric high voltage DC cable insulation, Ph.D. thesis, T. U. Delft, The Netherlands, 2006.

Boggs, S., A rational consideration of space charge, IEEE Electrical Insulation Magazine, 20, pp. 22-27, 2004.

Boggs, S., Damon, D. H., Hjerrild, J., Holboll, J. T., and Henriksen, M., Effect of insulation properties on field grading of solid dielectric DC cables, IEEE Trans. Power Delivery, 16, pp. 456-461, 2001.

Boström, J. O., Campus, A., Hampton, R. N., and Nilsson, U. H., Evaluation of the material reliability for polymeric direct current cables, Cigré, 15-404, 2002.

Chong, Y. L., Chen, G., and Ho, Y. F. F., Temperature effect on space charge dynamics in XLPE insulation, IEEE Trans. Dielectrics and Electrical Insulation, 14, pp. 65-76, 2007.

Dissado, L. A. and Fothergill, J. C., Electrical degradation and breakdown in polymers, Peter Peregrinus Ltd, UK, 1992.

Hanley, T. C., Burford, R. P., Fleming, R. J., and Barber, K. W., A general review of polymeric insulation for use in HVDC cables, IEEE Electrical Insulation Magazine, 19, pp. 13-24, 2003.

Ildstad, E., Sletbak, J., Nyberg, B. R., and Larsen, J. E., Factors affecting the choice of insulation system for extruded HVDC power cables, Cigré, D1-203, 2004.

Lau, H., Aufbau der Raumladung in einem betriebswarmen Gleichspannungskabel, Archiv für Elektrotechnik, 53, pp. 265-275, 1970.

Lewis, T. J., Polyethylene under electrical stress, IEEE Trans. Dielectrics and Electrical Insulation, 9, pp. 717-729, 2002.

Olsson, C. O., Diffusion in polymers with temperature dependent properties, paper MST-01, 13th Int. Heat Transfer Conf., Aug. 13-18, Sydney, NSW, Australia, 2006.

Pugliese, E., La répartition transversale de la tension alternative et continue dans l'isolant des cables à haute tension, S.E.V. Bulletin, 41, pp. 921-925, 1950.

Tellier, R., Constantin, L., and Brenac, J. M., Recherches et progrès récents dans la technique des cables à courant continue et à courant alternatif à haute tension, CIGRE report 212, 1958.